

Validation of rotary cone penetration test for soil interface frictional coefficient estimation

Xiaotong Yang, Jian-Min Zhang, Rui Wang

Department of Hydraulic Engineering, Tsinghua University, Beijing 100084, China; yangxiaotong20@outlook.com

ABSTRACT: The cone penetration test (CPT) is a widely used in-situ technique for soil characterization, but its effectiveness is often limited in high-resistance soils due to insufficient penetration capability. Recent studies have demonstrated that rotary CPT enhances penetration performance while also providing additional information through torque measurements. One of the key applications of the additional measured torque on the cone (t_c) is its combined use with the vertical cone resistance (q_c) to estimate the soil-structure interface friction coefficient based on a theoretical derivation. This study employs discrete element method (DEM) to simulate rotary cone penetration test. q_c and t_c are measured under varying cone surface friction conditions, enabling the calculation of the soil-cone interface friction coefficient. Complementary DEM ring shear tests were conducted to determine the true soil-structure interface friction coefficient, allowing validation against rotary CPT-derived estimates. The results show that both q_c and t_c increase with higher predefined friction coefficients, though t_c exhibits a more pronounced response due to differences in their governing mechanisms. The findings in this study confirm that rotary CPT can effectively estimate the interface friction coefficient by analyzing the relationship between q_c and t_c . However, the accuracy of the estimation is higher for smoother interfaces ($\mu < 0.23$), while rougher interfaces lead to slight underestimation. This study provides critical validation for the application of rotary CPT in estimating soil-structure friction properties.

KEYWORDS: Rotary CPT, Ring shear test, Soil-structure interface friction coefficient.

1 INTRODUCTION

The Cone penetration test (CPT) is an important in situ testing tool, valued for its quick, reliable, and continuous soil characterization (Arroyo et al., 2011). To overcome the low penetrability of CPT in hard soils that often restricts its application in deep stratigraphic investigations (Sani et al., 2019; Zhang et al., 2019), existing solutions include lubricating the soil-probe interface by injecting water or drilling fluid around the rods (Jefferies and Funegard, 1983) or directly at the cone tip (Yetginer-Tjelta et al., 2022). However, fluid injection may cause soil disturbance, potentially compromising CPT data accuracy. Alternatively, researchers have explored extended probe motions to enhance CPT performance and applicability, including cyclic CPT (Diambra et al., 2014), vibro-CPT (Stähler et al., 2018), circumnutation-inspired penetration (Anilkumar and Martinez, 2024, 2025), and rotary CPT (White, 2022).

Among these methods, rotary CPT offers a simple yet effective solution by introducing an additional rotational motion alongside conventional penetration. This quasi-static in situ approach not only minimally disturbs the soil structure but also enables torque measurement. Multiple studies have confirmed that rotation improves CPT penetrability by reducing both tip resistance and sleeve friction (Del Dottore et al., 2017; Tang and Tao, 2022; Yang et al., 2023, 2024a). The underlying resistance reduction mechanism has been elucidated through theoretical analyses (Bengough et al., 1997; Song et al., 2011; Yang et al., 2024a) and microscale observations (Sharif et al., 2021; Tang and Tao, 2021; 2022). Yang et al. (2024a) attribute the resistance reduction to two factors: (1) the decrease in normal contact forces at the interface; (2) the reorientation of interface friction from vertical towards horizontal directions.

Existing research provides a foundation for extending the applications of rotary cone penetration testing (CPT) to soil property estimation, e.g., shear strength, liquidity index, and consolidation coefficient (White 2022). Besides, accurate estimation of soil-structure interface friction characteristics requires both normal and tangential force data on the same contact surface. Conventional cone penetration tests (CPT) cannot achieve this, as their measurements (cone resistance and sleeve friction) are taken separately. In contrast, rotary CPT simultaneously records vertical force and torque resistance at

the cone, providing paired normal and tangential force data. This capability allows direct estimation of the interface friction coefficient (Bengough et al., 1997; Song et al., 2011; Yang et al., 2024b). To rigorously evaluate rotary CPT's effectiveness on estimating the interface friction property, this study employs DEM simulations of rotary CPT test to obtain cone-specific vertical and torque resistances for calculating the interface friction coefficient, complemented by DEM ring shear tests to establish true interface friction coefficients. The benchmark values enable a systematic comparison with rotary CPT-derived estimates, offering new insights into the method's reliability for interface friction characterization.

2 TEST METHODS AND MATERIALS

2.1 Rotary CPT test

The DEM code PFC3D is employed in this study to simulate rotary CPT penetration in a virtual calibration chamber (Figure 1). The 3D cylindrical model, with a diameter of 0.432 m and height of 0.7 m, was constructed following Arroyo et al. (2011)'s methodology. To minimize boundary effects, all chamber walls were assigned frictionless contacts. The penetration probe consisted of a 60° apex cone and a rod shaft with a diameter (d_c) of 0.036 m. Particle sizes in the central cylindrical region were scaled up by a factor of 39, resulting in a median particle diameter (d_{50}) of 8.19 mm, compared to the real soil's d_{50} of 0.21 mm (Figure 2). Multi-scaling method (Mcdowell et al., 2012) upscales particle sizes with scaling factors gradually increasing from the chamber center to the outer boundary. This approach was used to generate the specimen with a manageable number of particles and sufficient contacts with the probe. This yielded a cone/particle ratio (d_c/d_{50}) of 4.4 and a chamber/cone ratio of 12, exceeding typical values in prior 3D penetration studies (Chen et al., 2021) and ensuring minimal boundary and scale effects on the results.

Fontainebleau sand (Yang et al., 2010) was simulated using a rough Hertzian contact model that accounts for surface roughness effects. The contact parameters were calibrated based on Zhang et al. (2021). The shear modulus (G) was set to 32 GPa and the Poisson's ratio (ν) to 0.19. Particle rotation was inhibited to approximate the behavior of non-spherical particles (Calvetti, 2008). The probe surface had an initial friction

coefficient of 0.275, matching that of the particles. We also performed another ten simulations with varied probe frictional coefficients (0.05-0.26) to evaluate the effectiveness of rotary CPT in estimating the soil-probe interface frictional coefficient. Prior to penetration, the specimen was under isotropic conditions. All simulations used a local damping coefficient of 0.05 (Cundall, 1987), with no viscous damping.

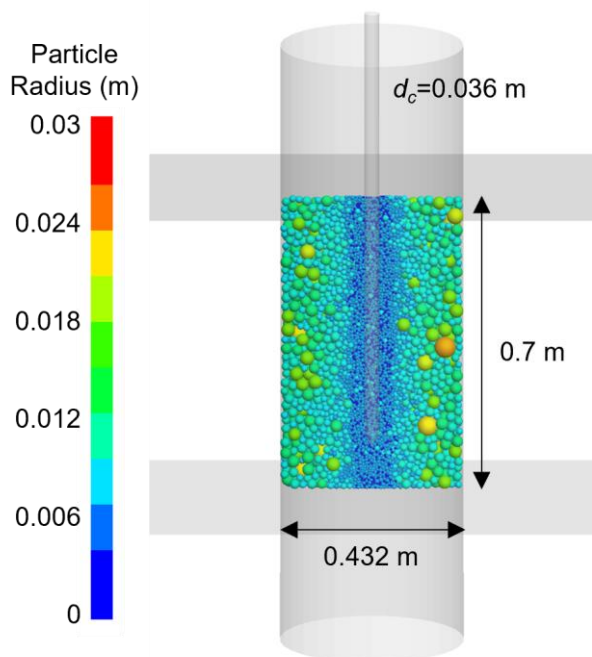


Figure 1. A side view of the DEM model of Rotary CPT test.

To achieve the target relative density, specimens were generated using the radius expansion method by varying the initial number of particles. After expansion, the inter-particle friction coefficient was temporarily reduced to 0.05, followed by isotropic compression at 5 kPa for pre-confining. The friction coefficient was then reset to the calibrated value, and confining stress was gradually increased to the target level of 800 kPa on the radial, top, and bottom walls using a servo-controlled mechanism. Specimens were prepared with an initial void ratio (e) of 0.621, corresponding to a relative density (D_r) of 71.6%, based on $e_{max}=0.9$ and $e_{min}=0.51$ (Ciantia et al., 2019).

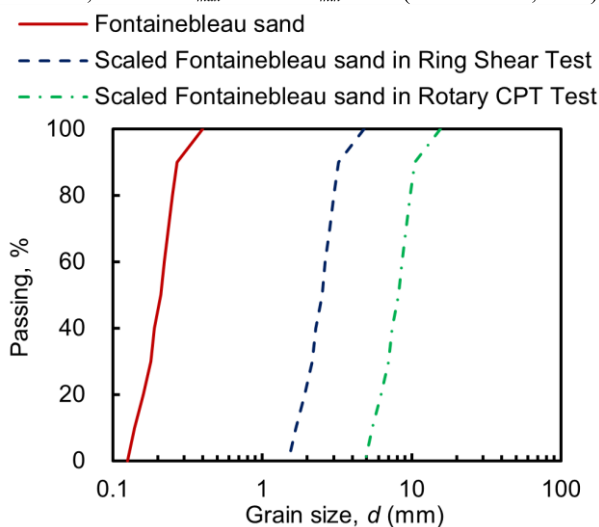


Figure 2. Particle size distribution of the tested materials (Fontainebleau sand and its upscaled particles used in the DEM models).

During penetration tests, the top and bottom walls were servo-controlled to maintain confining pressures of 800 kPa, while the bottom wall remained fixed. The DEM model facilitated the analysis of rotary CPT behavior under high-stress conditions. To optimize computational efficiency, a vertical penetration velocity (v) of 0.5 m/s was used. To avoid penetration or rotation motion dominating excessively, a rotation speed ω of 27.78 rad/s was set in the rotary CPT, with the speed ratio between rotation and penetration $SR=(\omega d_c/2)/v$ being 1.

2.2 Ring shear test

The DEM-simulated ring shear test employed the same Fontainebleau sand material used in the rotary CPT simulations, with a scaling factor of 12 applied to ensure sufficient particle resolution (~24,000 particles within the hollow cylindrical chamber, see Figure 3). Sample preparation followed the radius expansion method to achieve identical density conditions as in the rotary CPT tests. After initial specimen generation, a stepwise vertical stress was applied: beginning at 5 kPa, then incrementing to 50 kPa, followed by 100 kPa increments (stabilizing at each step) until a final consolidation stress of 800 kPa was reached. This progressive loading ensured proper particle rearrangement and reliable contact between the specimen and the chamber.

The top plate was horizontally constrained and servo-controlled to maintain a constant vertical stress of 800 kPa during shearing. To enhance the interface roughness, twelve stationary baffle plates, fixed to the top plate, were embedded into the specimen. Shear loading was applied by rotating the bottom plate at a rate of 10°/s, higher than the recommended rates in Rui et al. (2021) and Tan et al. (1998) for physical tests, but justified by prior parametric studies confirming numerical stability while maintaining computational efficiency. The frictional resistance at the bottom boundary was modeled by adjusting the wall-particle contact friction coefficient ($\mu = 0.05 - 0.275$). Torque evolution during shearing was monitored at the top surface.

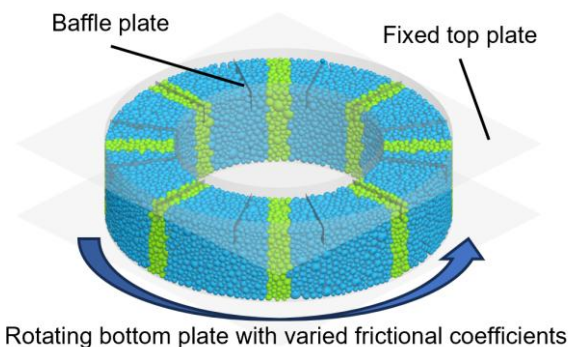


Figure 3. DEM model of the ring shear test.

3 TEST RESULTS

3.1 Rotary CPT test results

During rotary penetration in the DEM-calibrated chamber, the evolution of vertical cone resistance (q_c) and cone torque (t_c) was recorded to characterize soil-probe interactions. Figure 4 presents the measured and fitted results for three selected cone-surface friction coefficients ($\mu = 0.05, 0.17, \text{ and } 0.275$). Consistent with Yang et al. (2024a), both q_c and t_c stabilize around constant values beyond a penetration depth of 0.15 m. However, the raw data exhibit fluctuations due to the scaled particle size. To extract the underlying trends while filtering noise, the raw signals were processed using the exponential

fitting method proposed by Arroyo et al. (2011), yielding smoothed steady-state values for deeper penetration that were used in subsequent analyses.

The friction coefficient μ significantly affects both q_c and t_c . Increasing μ from 0.05 to 0.17 and 0.275 raises q_c by 15.2 MPa and 27.7 MPa (~23% and 42% increases, respectively), whereas t_c increases by 116 N·m and 210.9 N·m (~213% and 388% increases, respectively). This disproportionate enhancement in t_c arises because it is composed mainly by tangential force and scales nearly linearly with μ , while q_c is governed primarily by normal contact forces, which remain less sensitive to μ (Yang et al., 2024a). The contrasting responses of q_c and t_c under varying μ enable back-calculation of the cone-sand friction coefficient in rotary CPT testing by combining both measurements.

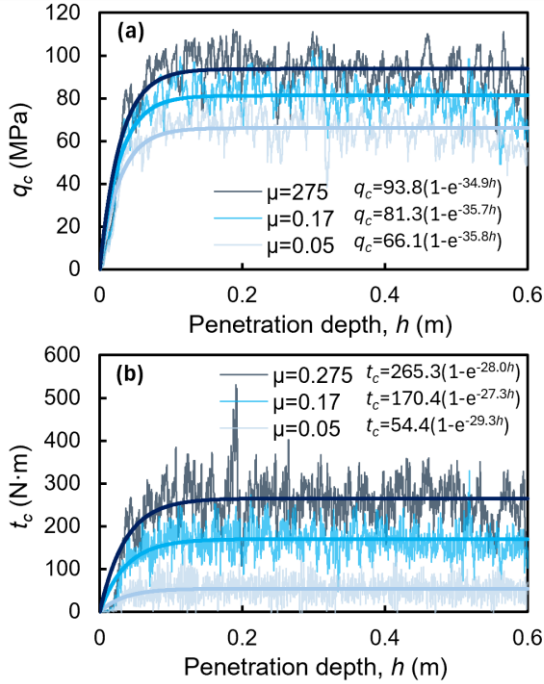


Figure 4. Measured and fitted results from Rotary CPT showing the relationship between penetration depth and (a) vertical tip resistance (q_c) and (b) cone torque (t_c) for different cone-surface friction coefficients (μ).

3.2 Ring shear test results

The ring shear test measures three primary parameters: mean vertical normal stress (σ_n), mean shear stress (τ_n), and mean shear displacement (S). These are calculated using the following expressions:

$$\sigma_n = \frac{w}{\pi(R_o^2 - R_i^2)} \quad (1)$$

$$\tau_n = \frac{3M}{2\pi(R_o^3 - R_i^3)} \quad (2)$$

$$S = \theta R_m = \theta \frac{D_o^3 - D_i^3}{3(D_o^2 - D_i^2)} \quad (3)$$

Figure 5 presents the relationship between shear stress (τ_n) and shear displacement (S) for varying base-plate friction coefficients. The results demonstrate that the magnitude of τ_n increases monotonically with higher μ . τ_n initially rises with shear displacement, reaches a peak value, and subsequently exhibits slight strain-softening behavior.

The peak shear stress value was adopted to determine the interface friction coefficient in the ring shear tests as $\mu_0 = \tau_n^{peak}/\sigma_n$. This approach captures the critical stress state at which interface failure occurs.

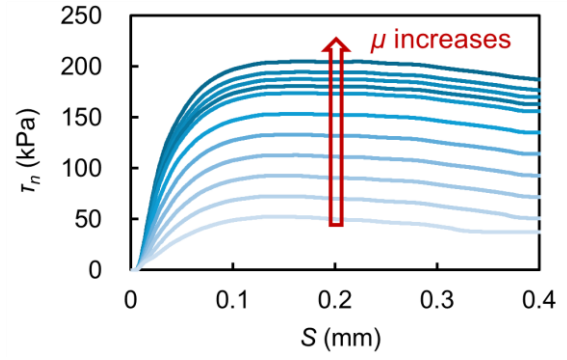


Figure 5. Relationship between mean shear stress (τ_n) and mean shear displacement (S) in ring shear tests using bottom plates with different surface friction coefficients (μ).

4 PREDICTING THE FRICTIONAL COEFFICIENT USING ROTARY CPT TEST

As derived in Yang et al. (2024b), the vertical resistance on cone in rotary CPT q_c can be calculated as equation (4):

$$q_c = \sigma_r (1 + \sqrt{3}\mu\delta_{qc}) \quad (4)$$

where, q_c and σ_r are the tip resistance and unit area normal force acted on the cone surface respectively; δ_{qc} is the influence factor of rotation on frictional force, as a function of penetration velocity, rotation velocity, and cone diameter.

$$\delta_{qc} = \frac{\sqrt{3}}{\sqrt{\frac{d_c^2}{4} \left(\frac{\omega}{v}\right)^2 + \frac{3}{4} + \frac{\sqrt{3}}{2}}} \quad (5)$$

t_c can be derived as:

$$t_c = \frac{\sigma_r \mu \delta_{tc}}{4} \quad (6)$$

where δ_{tc} is the influence factor of rotation on torque resistance (Song et al., 2011):

$$\delta_{tc} = \frac{16}{3} \left[1 - \frac{6}{d_c^2} \left(\frac{v}{\omega}\right)^2 \right] \sqrt{\frac{d_c^2}{4} + \frac{3}{4} \left(\frac{v}{\omega}\right)^2} + \frac{16\sqrt{3}}{d_c^2} \left(\frac{v}{\omega}\right)^3 \quad (6)$$

As per equations (4) and (6), the soil-probe friction coefficient (μ') can be calculated using the measured q_c and t_c from rotary CPT with the following equation:

$$\mu' = \frac{4}{(q_{c,r}/t_c) \delta_{tc} - 4\sqrt{3}\delta_{qc}} \quad (7)$$

Figure 6 compares μ' (estimated from rotary CPT) with the peak friction coefficient (μ_0) measured in ring shear tests, including reference lines to assess their alignment. The results demonstrate that μ' estimates μ_0 with reasonable accuracy, maintaining errors within 10% across the tested range ($\mu_0=0.05-0.275$). Specifically, the predictions (μ') align closely with measured values for $\mu_0 < 0.23$, while increasing deviations were observed beyond $\mu_0 > 0.23$. The analysis suggests that when μ_0 exceeds 0.275, the discrepancy may keep increasing and requires further investigation, though such analysis is currently constrained by model limitations. This trend aligns with Yang et al. (2024b), where the underestimation is attributed to the breakdown of theoretical assumptions, particularly when soil no longer remains stationary during penetration. A rougher probe surface promotes particle rotation alongside the cone, skewing friction measurements, as confirmed by particle-scale observations. Generally, rotary CPT test provides a largely reliable estimation of the soil-cone interface friction coefficient, which could be utilized in practice such as pile installation.

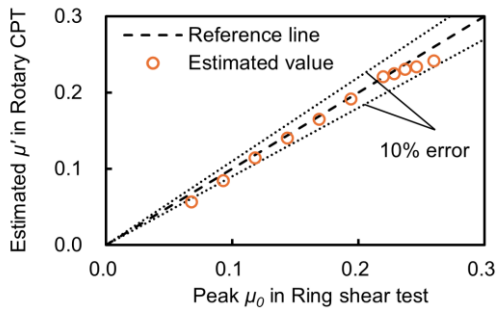


Figure 6. Correlation between the estimated friction coefficient from Rotary CPT and the measured value in ring shear tests.

5 CONCLUSIONS

This study performs eleven discrete element method (DEM) simulations of rotary cone penetration tests (CPT) alongside eleven corresponding ring shear tests with varying interfacial friction coefficients. The vertical cone resistance (q_c) and cone torque (t_c) are used to calculate the cone-soil interfacial friction coefficient and compared with values measured in ring shear tests.

Rotary CPT tests show that both cone resistance (q_c) and torque resistance (t_c) increase significantly with the set friction coefficient. However, t_c exhibits a more pronounced increase than q_c , attributable to their dominant dependence on tangential and normal interface contact forces, respectively. As a result, rotary CPT can reliably estimate the interfacial friction coefficient using q_c and t_c measurements. The estimations are accurate for smoother interfaces ($\mu < 0.23$) but progressively underestimate μ for rougher surfaces.

A modeling limitation stems from the model settings, where the interfacial friction coefficient is determined by the smaller value of the probe and particle friction coefficients. Because this study fixed the particle surface friction coefficient, it could not simulate conditions with higher interfacial friction, restricting the investigation of rougher interface behavior. Future work should broaden the insights in such scenarios. Additionally, physical model tests should be conducted to validate rotary CPT's friction coefficient calculations, enhancing its development and field application. Improved interpretation methods for rotary CPT data are also crucial for practical implementation and warrant future investigation.

6 ACKNOWLEDGEMENTS

The financial support of the National Natural Science Foundation of China (No. 52378349 and 52425904) is acknowledged.

7 REFERENCES

Anilkumar, R., & Martinez, A. 2024. Experimental investigation of circumnutation-inspired penetration in sand. *Bioinspiration & Biomimetics*, 20(1), 016006.

Anilkumar, R. and Martinez, A., 2025. Plant Root-inspired Penetration Experiments in Layered Sand Profiles.

Arroyo, M., Butlanska, J., Gens, A., Calvetti, F. and Jamiolkowski, M., 2011. Cone penetration tests in a virtual calibration chamber. *Géotechnique*, 61(6), pp.525–531.

Bengough, A.G., Mullins, C.E. and Wilson, G., 1997. Estimating soil frictional resistance to metal probes and its relevance to the penetration of soil by roots. *European Journal of Soil Science*, 48(4), pp.603–612.

Calvetti, F., 2008. Discrete modelling of granular materials and geotechnical problems. *European Journal of Environmental and Civil Engineering*, 12(7–8), pp.951–965.

Chen, Y., Khosravi, A., Martinez, A. and DeJong, J., 2021. Modeling the self-penetration process of a bio-inspired probe in granular soils. *Bioinspiration & Biomimetics*, 16(4), p.046012.

Ciantia, M.O., Arroyo, M., O'Sullivan, C., Gens, A. and Liu, T., 2019. Grading evolution and critical state in a discrete numerical model of Fontainebleau sand. *Géotechnique*, 69(1), pp.1–15.

Cundall, P.A., 1987. Distinct element models, of rock and soil structure. *Analytical and computational method in engineering rock mechanics*, pp.129–1631.

Del Dottore, E., Mondini, A., Sadeghi, A., Mattoli, V. and Mazzolai, B., 2017. An efficient soil penetration strategy for explorative robots inspired by plant root circumnutation movements. *Bioinspiration & biomimetics*, 13(1), p.015003.

Diambra, A., Ciavaglia, F., Harman, A., Dimelow, C., Carey, J. and Nash, D.F.T., 2014. Performance of cyclic cone penetration tests in chalk. *Géotechnique Letters*, 4(3), pp.230–237.

Jefferies, M.G. and Funegard, E., 1983. Cone penetration testing in the Beaufort Sea. In: *Geotechnical Practice in Offshore Engineering*. ASCE. pp.220–243.

Mcdowell, G.R., Falagush, O. and Yu, H.-S., 2012. A particle refinement method for simulating DEM of cone penetration testing in granular materials. *Géotechnique Letters*, 2(3), pp.141–147.

Rui, S., Wang, L., Guo, Z., Zhou, W., & Li, Y. (2021). Cyclic behavior of interface shear between carbonate sand and steel. *Acta Geotechnica*, 16(1), 189-209.

Sani, A.K., Singh, R.M., Amis, T. and Cavarretta, I., 2019. A review on the performance of geothermal energy pile foundation, its design process and applications. *Renewable and Sustainable Energy Reviews*, 106, pp.54–78.

Sharif, Y.U., Brown, M.J., Ciantia, M.O., Cerfontaine, B., Davidson, C., Knappett, J., Meijer, G.J. and Ball, J., 2021. Using discrete element method (DEM) to create a cone penetration test (CPT)-based method to estimate the installation requirements of rotary-installed piles in sand. *Canadian Geotechnical Journal*, 58(7), pp.919–935.

Song, L., Feng-Yin, L. and Li, N., 2011. On mechanism of rotary cone penetration test. *Rock and Soil Mechanics*, 32(S1), pp.787–792.

Stähler, F.T., Kreiter, S., Goodarzi, M., Al-Sammarrhaie, D. and Mörz, T., 2018. Liquefaction resistance by static and vibratory cone penetration tests. In: *Cone Penetration Testing 2018*.

Tan, S. A., Chew, S. H., & Wong, W. K. (1998). Sand-geotextile interface shear strength by torsional ring shear tests. *Geotextiles and Geomembranes*, 16(3), 161-174.

Tang, Y. and Tao, J., 2021. Effect of Rotation on Penetration: Toward a Seed Awn-Inspired Self-Burrowing Probe. In: *IFCEE 2021. [online] International Foundations Congress and Equipment Expo 2021*. Dallas, Texas: American Society of Civil Engineers. pp.149–159.

Tang, Y. and Tao, J., 2022. Multiscale analysis of rotational penetration in shallow dry sand and implications for self-burrowing robot design. *Acta Geotechnica*, 17(10), pp.4233–4252.

White, D.J., 2022. CPT equipment: Recent advances and future perspectives. *Cone Penetration Testing 2022*, pp.66–80.

Yang, X., Zhang, N., Wang, R., Martinez, A., Chen, Y., Fuentes, R. and Zhang, J.-M., 2024a. A numerical investigation on the effect of rotation on the cone penetration test. *Canadian Geotechnical Journal*, 61(11), pp.2468–2484.

Yang, X., Zhang, N., Wang, R., Zhang, J.-M., Fuentes, R. and Zhang, W., 2023. DEM modelling of a rotary CPT. In: *ISSMGE*.

Yang, X., Zhang, N., Zhang, J.-M. and Wang, R., 2024b. Discrete element modelling of rotary CPT and its applications. *Computers and Geotechnics*, 170, p.106332.

Yang, Z.X., Jardine, R.J., Zhu, B.T., Foray, P. and Tsuha, C.H.C., 2010. Sand grain crushing and interface shearing during displacement pile installation in sand. *Géotechnique*, 60(6), pp.469–482.

Yetginer-Tjelta, T.I., Botker-Rasmussen, S., Rose, M., Lunne, T., Meyer, V. and Duffy, C., 2022. Development of an enhanced CPT system for Dogger Bank. In: *Cone Penetration Testing 2022*.

Zhang, N., Arroyo, M., Ciantia, M.O., Gens, A. and Butlanska, J., 2019. Standard penetration testing in a virtual calibration chamber. *Computers and Geotechnics*, 111, pp.277–289.

Zhang, N., Ciantia, M.O., Arroyo, M. and Gens, A., 2021. A contact model for rough crushable sand. *Soils and Foundations*, 61(3), pp.798–814.